A

	Rbd1	Rbd2	Rbd3	Rbd4	Rbd5	Rbd6	Rbd7	Rbd8	Rbd9	Rbd10	Rbd11	Rbd12
Rbd1	-	9271	361	65	2068	1948	571	1427	1497	0	933	0
Rbd2	9271	-	1710	125	46	92	114	5	1381	1507	420	999
Rbd3	361	1710	-	0	0	0	0	171	0	1084	2043	587
Rbd4	65	125	0	-	0	0	2135	0	0	0	0	0
Rbd5	2068	46	0	0	-	130	0	0	0	0	0	0
Rbd6	1948	92	0	0	130	-	462	0	0	0	0	0
Rbd7	571	114	0	2135	0	462	-	0	0	0	0	0
Rbd8	1427	5	171	0	0	0	0	-	0	0	188	0
Rbd9	1497	1381	0	0	0	0	0	0	-	0	0	0
Rbd10	0	1507	1084	0	0	0	0	0	0	-	0	74
Rbd11	933	420	2043	0	0	0	0	188	0	0	-	14
Rbd12	0	999	587	0	0	0	0	0	0	74	14	-

B

	Rbd1	Rbd2	Rbd3	Rbd4	Rbd5	Rbd6	Rbd7	Rbd8	Rbd9	Rbd10	Rbd11	Rbd12
Rbd1	-	1	1	0	1	1	1	1	1	0	1	0
Rbd2	1	-	1	0	0	0	0	0	1	1	1	1
Rbd3	1	1	-	0	0	0	0	0	0	1	1	1
Rbd4	0	0	0	-	0	0	1	0	0	0	0	0
Rbd5	1	0	0	0	-	0	0	0	0	0	0	0
Rbd6	1	0	0	0	0	-	1	0	0	0	0	0
Rbd7	1	0	0	1	0	1	-	0	0	0	0	0
Rbd8	1	0	0	0	0	0	0	-	0	0	0	0
Rbd9	1	1	0	0	0	0	0	0	-	0	0	0
Rbd10	0	1	1	0	0	0	0	0	0	-	0	0
Rbd11	1	1	1	0	0	0	0	0	0	0	-	0
Rbd12	0	1	1	0	0	0	0	0	0	0	0	-

C

	Rbd1	Rbd2	Rbd3	Rbd4	Rbd5	Rbd6	Rbd7	Rbd8	Rbd9	Rbd10	Rbd11	Rbd12
Rbd1	-	14	0	3	6	8	1	0	2	0	4	0
Rbd2	14	-	2	1	0	0	0	0	0	3	0	3
Rbd3	0	2	-	0	0	0	0	0	0	4	1	2
Rbd4	3	1	0	-	2	1	2	0	0	0	0	0
Rbd5	6	0	0	2	-	5	0	0	0	0	0	0
Rbd6	8	0	0	1	5	-	1	0	0	0	0	0
Rbd7	1	0	0	2	0	1	-	0	0	0	0	0
Rbd8	0	0	0	0	0	0	0	-	0	0	0	0
Rbd9	2	0	0	0	0	0	0	0	-	0	0	0
Rbd10	0	3	4	0	0	0	0	0	0	-	0	0
Rbd11	4	0	1	0	0	0	0	0	0	0	-	0
Rbd12	0	3	2	0	0	0	0	0	0	0	0	-

Supplemental Figure 2. Defining adjacency of interacting yeast RNAP subunits in PDB 1WCM from cross-links identified by Chen et al. (24). Summary of data calculated from known crystal structure and reported cross-link data RNA Polymerase II complex (24). A, the size of the intersubunit interface (in $Å^2$) for each pair of subunits in the experimental structure of the twelve subunit RNA polymerase II structure complex (PDB 1WCM). The interface area for a pair of subunits is calculated using the solvent accessible surface area (SASA) of the monomers and the dimer by: [[SASA(A)+SASA(B)]−SASA(AB)]/2. B, topology matrix calculated using a threshold of 250 $Å^2$ to define adjacency (note that this matrix is equivalent to a graph structure). C, observed unique lysine-lysine interlinks for RNAPII complex (24). Using the adjacency matrix in panel B, 53 of 65 cross-links is determined to come from adjacent pairs corresponding to an estimate of $p = 0.82$.

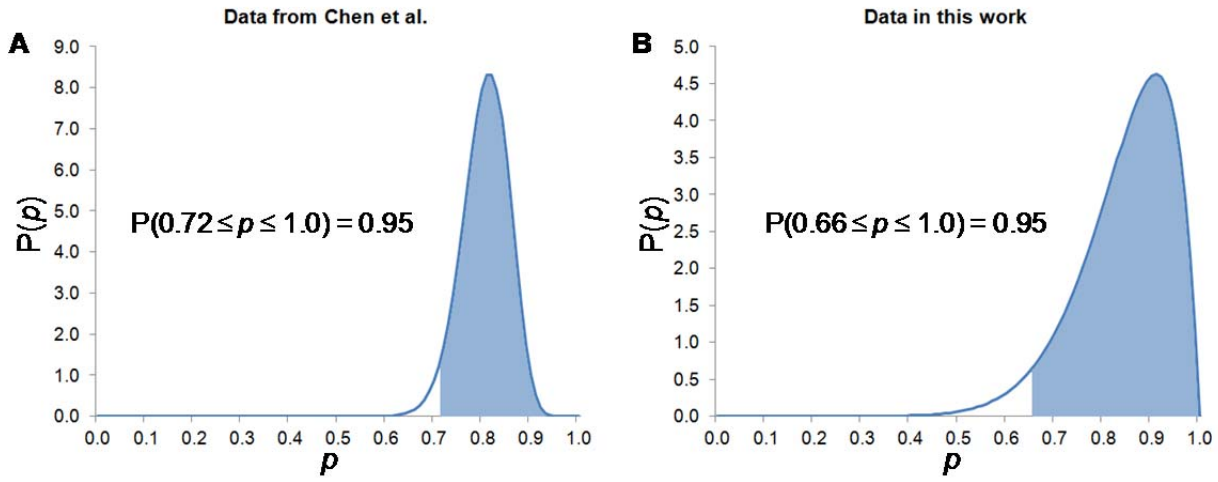

Supplementary Figure 3. Determining the optimal p-value for use in modeling of the 19S topology. A-B, probability density functions (PDF) and confidence intervals for the global parameter *p*. Probability density function and the associated confidence interval were calculated using cross-linking data from RNAPII (24) in panel A and the 19S ATPase base ring in this work in panel B. For both datasets the number of unique lysine-lysine interlinks were used. A, twelve subunit experimental structure of RNAPII – with subunit adjacency defined by a shared interface of at least 250 $Å^2$ (Supplemental Figure 2), the published crosslink data from Chen et al. (24) results in an observed count of 53/65 cross-links coming from adjacent subunits. B, the 19S RP base hexamer under the assumption that the proposed base subunit ordering is correct; the observed count of 10/11 is used to parameterize the beta distribution and generate the PDF and confidence intervals.

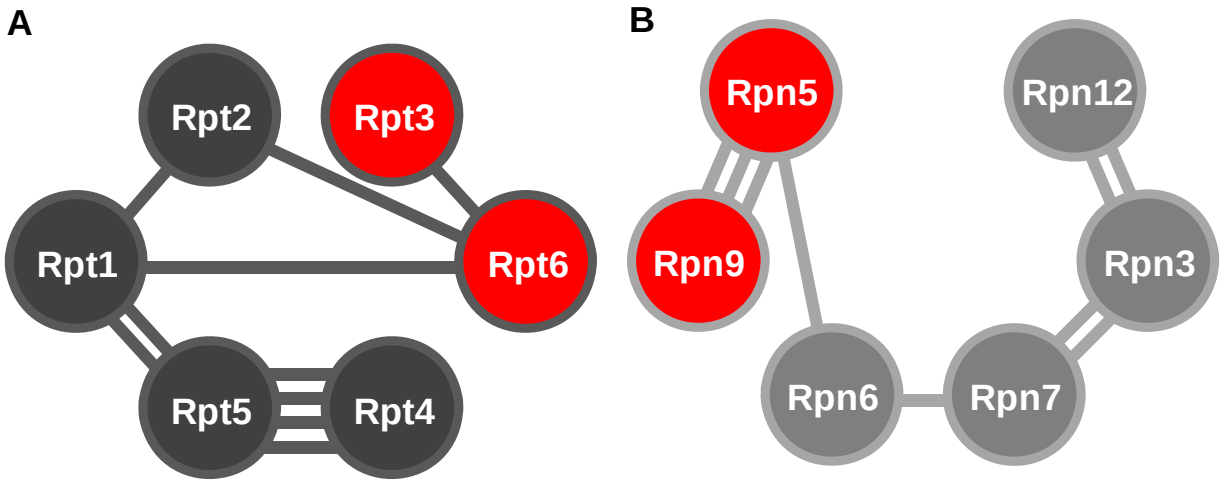

Supplemental Figure 4. The second most likely (G_{ML2}) ordering for the ATPase base heterohexamer (A) and the PCI domain-containing heterohexamer (B). A, the G_{ML2} graph for the base ring has only a single ordering as Rpt1-2-3-6-4-5, corresponding to a switch of subunits Rpt3 and Rpt6 with respect to G_{ML} (Rpt 1-2-6-3-4-5). This G_{ML2} ordering results in violations of two cross-link constraints: Rpt2-6 and Rpt1-6. B, throughout the range of p values, there are six possible orderings of PCI domain-containing hexamer representing the G_{ML2} graph, i.e. Rpn5-9-6-7-3-12 (*shown above*), Rpn9-5-6-12-3-7, Rpn9-5-12-3-7-6, Rpn5-9-12-3-7-6, Rpn6-5-9-7-3-12, and Rpn6-5-9-12-3-7. In comparison to the G_{ML} ordering (Rpn9-5-6-7-3-12) which does not have any constraint violation, each of these G_{ML2} graph violates one cross-link constraint: Rpn5-6 or Rpn6-7 (subunits underlined above). The unique lysine-lysine linkages between subunits are shown.

A

	A	G	Z	Q	H	E	B	D
A	-	2	0	0	0	0	0	2
G	2	-	9	0	0	0	0	0
Z	0	9	-	7	0	0	0	0
Q	0	0	7	-	1	0	0	0
H	0	0	0	1	-	0	0	0
E	0	0	0	0	0	-	1	1
B	0	0	0	0	0	1	-	3
D	2	0	0	0	0	1	3	-

B

	A	G	Z	Q	H	E	B	D
A	-	1	0	0	0	0	0	1
G	1	-	1	0	0	0	0	0
Z	0	1	-	1	0	0	0	0
Q	0	0	1	-	1	0	0	0
H	0	0	0	1	-	1	0	0
E	0	0	0	0	1	-	1	0
B	0	0	0	0	0	1	-	1
D	1	0	0	0	0	0	1	-

C

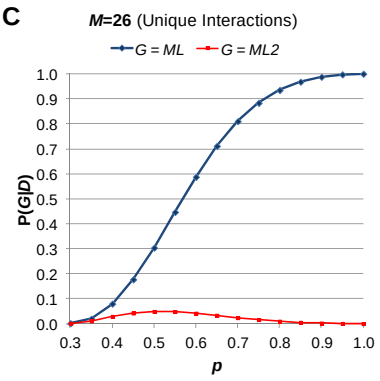

Supplementary Figure 5. Probabilistic analysis of cross-linking data obtained from eukaryotic TRiC/CCT chaperonin complex by Kalisman et al. (45). A, counts of unique intersubunit cross-links obtained from Supplemental Table S1 from Kalisman et al. 2012. B, graph structure proposed in Kalisman et al. 2012, which matches the maximum likelihood graph (G_{ML}) from our probabilistic analysis. C, plot of the probability of G_{ML} and G_{ML2} as a function of the global parameter p. Note that while the combinatorial homology modeling approach of Kalisman et al. 2012 depends on homology models of each subunit, our approach is more general and can be applied in the absence of any structural information for individual subunits.